

1 **Estimating Transient Climate Response in a large-ensemble global climate model simulation**

2

3 B.K. Adams and A.E. Dessler\*

4 Dept. of Atmospheric Sciences, Texas A&M University, College Station, TX

5 \* corresponding author, [adessler@tamu.edu](mailto:adessler@tamu.edu)

6

7 Main points:

8 1. In a large model ensemble, we find that estimates of TCR from the 20<sup>th</sup> century tends to  
9 be low biased compared to the model's true TCR.

10 2. Internal variability can push down or enhance the warming in ensemble members &  
11 lead to large errors in TCR inferred from the 20<sup>th</sup> century.

12 3. We also verify that the details of the construction of the temperature dataset from  
13 which TCR is inferred can lead to significant biases in TCR inferred from observed  
14 warming.

15

16 **Plain language summary:**

17 The transient climate response (TCR) is defined to be the warming after 70 years of a 1% per  
18 year increase in atmospheric CO<sub>2</sub>. It is one of the important metrics in climate science because  
19 it plays a key role in determining how much warming we will experience in the future. Previous  
20 work has found that TCR inferred from observed warming over the 20th century tends to be  
21 lower than TCR in climate models. This has been used by suggest that climate models are  
22 overpredicting future warming. We use a large number of climate model runs to investigate  
23 the methodology of this comparison. We find that TCR estimated from the 20th century  
24 simulations may indeed be much lower than the model's true TCR. This arises from biases in  
25 the methodology of estimating TCR from 20th century warming, as well as biases in the  
26 construction of the observational temperature data sets. We therefore find no evidence that  
27 models are overestimating TCR.

28

29 **Abstract**

30 The transient climate response (TCR), defined to be the warming in near-surface air  
31 temperature after 70 years of a 1% per year increase in CO<sub>2</sub>, can be estimated from observed  
32 warming over the 19<sup>th</sup> and 20<sup>th</sup> centuries. Such analyses yield lower values than TCR estimated  
33 from global climate models (GCMs). This disagreement has been used to suggest that GCMs'  
34 climate may be too sensitive to increases in CO<sub>2</sub>. Here we critically evaluate the methodology  
35 of the comparison using a large ensemble of a fully coupled GCM simulating the historical  
36 period, 1850–2005. We find that TCR estimated from model simulations of the historical period  
37 can be much lower than the model's true TCR, replicating the disagreement seen between  
38 observations and GCM estimates of TCR. This suggests that the disagreement could be  
39 explained entirely by the details of the comparison and undercuts the suggestions that GCMs  
40 overestimate TCR.

41 **Introduction**

42 The transient climate response (TCR) is frequently used to quantify the sensitivity of our climate  
43 system to increases in greenhouse gases. It is defined to be the warming in near-surface air  
44 temperature after 70 years of a 1% per year increase in atmospheric CO<sub>2</sub>. As described below,  
45 it can be estimated from observed warming over the 19<sup>th</sup> and 20<sup>th</sup> centuries, yielding most-  
46 likely TCR values of 1.3-1.6 K [Bengtsson and Schwartz, 2013; Otto et al., 2013; Richardson et  
47 al., 2016; Lewis and Curry, 2018]. These values lie below the CMIP5 ensemble average TCR of  
48 1.8 K [Forster *et al.*, 2013]. This disagreement has been used to cast doubt on the fidelity of  
49 model simulations of future climate change.

50 We will test the methodology of this comparison using a large model ensemble, an increasingly  
51 popular tool to study the impact of internal variability on the climate system. The most  
52 appropriate ensemble for this type of problem contains many runs of a single model with  
53 identical physics and external forcing but different initial conditions. As each ensemble member  
54 evolves in time, internal variability of the different members is out of phase, leading to  
55 differences in the climate states among the ensemble members. In fact, one can think of our  
56 observational record as one member of a theoretical ensemble of Earth's climate trajectories.

57 A model ensemble therefore gives us insight into what alternative climate histories may have  
58 looked like.

## 59 **Data**

60 We analyze output from an ensemble of 100 runs of the fully-coupled Max Planck Institute  
61 Earth System Model version 1.1 (MPI-ESM1.1) covering the period 1850-2005. The ensemble  
62 was used by Dessler et al. [2018] to characterize the impact of internal variability on estimates  
63 of the equilibrium climate sensitivity (ECS); they found that internal variability can lead to  
64 significant errors in ECS inferred from historical observations. Hedemann et al. [2017] analyzed  
65 this ensemble to determine potential causes of the so-called warming hiatus that occurred in  
66 the 2000s.

67 As described by Dessler et al. [2018]: “This is the latest coupled climate model from the Max  
68 Planck Institute for Meteorology and consists of the ECHAM6.3 atmosphere and land model  
69 coupled to the MPI-OM ocean model. The atmospheric resolution is T63 spectral truncation,  
70 corresponding to about 200 km, with 47 vertical levels, whereas the ocean has a nominal  
71 resolution of about 1.5 degrees and 40 vertical levels. MPI-ESM1.1 is a bug-fixed and improved  
72 version of the MPI-ESM used during CMIP5 [Giorgetta *et al.*, 2013] and nearly identical to the  
73 MPI-ESM1.2 ... model being used to provide output to CMIP6, except that the historical forcings  
74 are from the MPI-ESM. Each of the 100 members simulates the years 1850-2005 (Fig. 1) and  
75 use the same evolution of historical natural and anthropogenic forcings. The members differ  
76 only in their initial conditions —each starts from a different state sampled from a 2000-year  
77 control simulation.”

78 Dessler et al. further say: “We calculate effective radiative forcing  $F$  for the ensemble by  
79 subtracting top-of-atmosphere flux  $R$  in a run with climatological sea surface temperatures  
80 (SSTs) and a constant pre-industrial atmosphere from average  $R$  from an ensemble of three  
81 runs using the same SSTs but the time-varying atmospheric composition used in the historical  
82 runs [Hansen *et al.*, 2005; Forster *et al.*, 2016]. The three-member ensemble begins with  
83 perturbed atmospheric states. We estimate  $F_{2\times\text{CO}_2}$  using the same approach in a set of fixed SST  
84 runs in which  $\text{CO}_2$  increases at 1% per year, which yields a  $F_{2\times\text{CO}_2}$  value of  $3.9 \text{ W/m}^2$ .”

85 We estimate  $F_{2\times\text{CO}_2}$  using the same approach in a set of fixed SST runs, one with a pre-industrial  
86 atmosphere and one in which  $\text{CO}_2$  increases at 1% per year. We estimate  $F_{2\times\text{CO}_2}$  as the average  
87 difference in top-of-atmosphere flux over years 62-78, which produces a value of  $3.7 \text{ W/m}^2$ .  
88 This is lower than the value used in Dessler et al. [2018],  $3.9 \text{ W/m}^2$ , which was estimated as  
89 one-half of the average over years 130-150. We feel the value of  $3.7 \text{ W/m}^2$  is a more  
90 appropriate estimate of  $2\times\text{CO}_2$  forcing in this model.

91 We will also analyze a 68-member ensemble of the MPI-ESM1.1 forced with  $\text{CO}_2$  increasing at  
92 1%/year (hereafter, “1% runs”). As with the historical ensemble, the 1% ensemble members  
93 differ only in their initial conditions — each starts from a different state sampled from a 2000-  
94 year pre-industrial control simulation.

## 95 **Analysis**

96 Time series of global-average near-surface air temperature for all 100 members are plotted in  
97 Fig. 1 of Dessler et al. [2018]; that plot shows that the model ensemble is in good agreement  
98 with observed surface temperatures. TCR can be estimated from the ensemble’s temperature  
99 data with this equation [Gregory and Forster, 2008; Otto *et al.*, 2013; Richardson *et al.*, 2016]:

$$100 \quad \text{TCR}_{hist} = \Delta T \frac{F_{2\times\text{CO}_2}}{\Delta F} \quad (1)$$

101 where  $\Delta T$  is the change in temperature over the historical period and  $\Delta F$  is the change in  
102 radiative forcing. In our analysis,  $\Delta$  represents the change between the 1859-1882 average,  
103 selected because it is not strongly influenced by volcanic eruptions [Mauritsen and Pincus,  
104 2017; Lewis and Curry, 2018], and the average of the last ten years of the runs, 1996-2005. We  
105 refer to TCRs estimated this way as  $\text{TCR}_{hist}$ .

106 We first calculate  $\text{TCR}_{hist}$  in each ensemble member using global-average near-surface air  
107 temperature for  $\Delta T$ . The calculated values range from 1.32 to 1.94 K (5-95% range 1.48-1.90 K)  
108 (Fig. 1a, Table 1). The spread in these TCR estimates is entirely due to internal variability and  
109 the spread is similar to previous estimates [Huber *et al.*, 2014; Hawkins *et al.*, 2016]. The  
110 standard deviation of  $\Delta T$  from the ensemble is 0.07 K, close to that assumed by Lewis and Curry  
111 [2015], implying a similar spread in TCR in their analysis.

112 TCR is formally defined as the warming of global-average near-surface air temperature in  
113 response to CO<sub>2</sub> increasing at 1% per year, at the time of doubling (year 70). This value, which  
114 we will call TCR<sub>true</sub>, can be estimated by averaging the warming (relative to pre-industrial) in  
115 year 70 of the 68-member ensemble of 1% runs. We find that TCR<sub>true</sub> for the MPI-ESM1.1 is  
116 1.81 K; this is 0.13 K (7.6%) larger than the average of the ensemble's TCR<sub>hist</sub> (1.68 K).

117 Thus, TCR<sub>hist</sub> is a low-biased estimate of TCR<sub>true</sub> in the ensemble. The magnitude, and even the  
118 sign, of this bias varies depending on the portion of the historical record being examined (Table  
119 1). Overall, though, we see a clear tendency for the TCR<sub>hist</sub> to underestimate TCR<sub>true</sub>. Previous  
120 papers have suggested that the biases in TCR<sub>hist</sub> could be due to aerosol forcing efficacy  
121 [Kummer and Dessler, 2014; Shindell, 2014; Marvel *et al.*, 2015], although that explanation  
122 remains to be validated in this ensemble.

123 We are now in a position to critically evaluate previous comparisons of TCR from observations  
124 and GCMs. TCR estimated from observations, which are TCR<sub>hist</sub>, have most-likely values in the  
125 range 1.3-1.6 K [Bengtsson and Schwartz, 2013; Otto *et al.*, 2013; Richardson *et al.*, 2016; Lewis  
126 and Curry, 2018], although the uncertainty in the individual estimates is large. The CMIP5  
127 ensemble's TCR, which are TCR<sub>true</sub>, fall in the range 1.8±0.6 K (average and 5-95% confidence  
128 interval) [Forster *et al.*, 2013]. Our analysis of the MPI-ESM1.1 ensemble demonstrates how a  
129 model with a TCR<sub>true</sub> of 1.81 K might nevertheless produce TCR<sub>hist</sub> in some ensemble members  
130 that that are much lower (1.3-1.4, Figure 1a) and in agreement with observational estimates.  
131 Thus, differences between observational TCRs and GCM TCRs could be mostly or entirely due to  
132 these issues.

133 We can also confirm previous suggestions that two issues with the observed ΔT, masking and  
134 blending, are further biasing TCR<sub>hist</sub> to even lower values [Richardson *et al.*, 2016]. Masking  
135 refers to the fact that the observations are geographically incomplete, and that the degree of  
136 incompleteness has changed over time, leading to biases in global-average ΔT [Cowtan and  
137 Way, 2014]. To test the impact of this on TCR<sub>hist</sub>, we also calculated ΔT in the ensemble using a  
138 time-varying mask derived from HadCRUT4 (v4.6.0.0) [Morice *et al.*, 2012]. Using this masked  
139 ΔT in Eq. 1, ensemble average TCR<sub>hist</sub> drops from 1.68 K to 1.59 K (Fig. 1b, Table 2).

140 The second issue is blending, which refers to the fact that observed  $\Delta T$  data sets are usually a  
141 blend of near-surface air temperature over land and sea ice but sea surface temperature (SST)  
142 over open ocean. Because near-surface air temperature is warming faster than SSTs, this  
143 blending lowers  $\Delta T$  compared to an estimate derived entirely from near-surface air  
144 temperature [Cowtan *et al.*, 2015; Santer *et al.*, 2000]. We test this by calculating a blended  $\Delta T$   
145 in the ensemble, which we also mask following HadCRUT4. Using this blended and masked  $\Delta T$ ,  
146 ensemble average  $TCR_{hist}$  drops to 1.47 K (Fig. 1d, Table 2). Importantly, none of the individual  
147 ensemble members have  $TCR_{hist}$  as large as the model's  $TCR_{true}$ .

148 Finally, we have also calculated blended  $\Delta T$  using the temperature of the model's top ocean  
149 layer (representing the top 12 m of the ocean) instead of SST. Using that estimate of  $\Delta T$ ,  $TCR_{hist}$   
150 drops even further, to an ensemble average of 1.44 K (Fig. 2f, Table 2).

## 151 **Conclusions**

152 We have investigated why observation-based estimates of TCR tend to be lower than those  
153 from GCMs using a perfect model experiment. We have quantified a number of biases that can  
154 explain most, if not all, of the disagreement: 1) a bias between  $TCR_{hist}$  and  $TCR_{true}$ , 2) a bias due  
155 to incomplete spatial coverage in the observational  $\Delta T$  record, and 3) a bias due to the  
156 observational  $\Delta T$  values being blends of air temperature and SSTs. These three biases are all  
157 acting in the same direction, to push  $TCR_{hist}$  to lower values. The impact of internal variability,  
158 which can suppress warming in some members of the ensemble, thereby further reducing  
159  $TCR_{hist}$ , is not yet quantifiable. But it has a potentially large magnitude and therefore could also  
160 be playing a role in the model-observation difference.

161 The uncertainty in individual estimates of  $TCR_{hist}$  from observations are large and the range  
162 easily covers most of the  $TCR_{true}$  values from the CMIP5 ensemble [Lewis and Curry, 2015; Lewis  
163 and Curry, 2018; Richardson *et al.*, 2016]. Because of the large uncertainty in other parameters  
164 (e.g., aerosol forcing), adding uncertainty due to the issues we discuss in this paper will produce  
165 only nominal increases in the total uncertainty of the observational estimates. However, the  
166 biases we have investigated are capable of explaining most or all of the disagreement between  
167 the central values of the estimates, which has been the focus of much of the discussion.

168 Our work also informs how future analyses should be done. First, analyses should account for  
169 the role of internal variability, most likely by comparing observations to an ensemble of runs. In  
170 addition, we should not compare  $TCR_{hist}$  derived from observations to  $TCR_{true}$  — unless one can  
171 quantify and adjust for the bias between these methods. A better approach would be to  
172 compare  $TCR_{hist}$  from observations to  $TCR_{hist}$  derived from an ensemble of runs of the GCMs  
173 covering the same period as the observations. Finally, one must account for biases in the  
174 observations of  $\Delta T$  due to masking and blending, most likely by calculating masked and blended  
175  $\Delta T$  fields from the model and using those to estimate the model-derived  $TCR_{hist}$ .

176

177 **Acknowledgments:** This work was supported by NSF grant AGS-1661861 to Texas A&M  
178 University. We thank the Bjorn Stevens, Thorsten Mauritsen, and Chris Hedemann of the Max-  
179 Planck-Institut für Meteorologie for their help interpreting output from the ensemble that  
180 formed the basis of this analysis. We also thank Mark Richardson for his suggestions on the  
181 manuscript. Data and code are available from [insert link after paper is accepted and code is  
182 finalized].

183

## 184 **References**

- 185 Bengtsson, L., & S. E. Schwartz (2013), Determination of a lower bound on Earth's climate  
186 sensitivity, *Tellus B: Chemical and Physical Meteorology*, 65, 21533, doi:  
187 10.3402/tellusb.v65i0.21533.
- 188 Cowtan, K., & R. G. Way (2014), Coverage bias in the HadCRUT4 temperature series and its  
189 impact on recent temperature trends, *Q. J. R. Meteor. Soc.*, 140, 1935-1944, doi:  
190 doi:10.1002/qj.2297.
- 191 Cowtan, K., Z. Hausfather, E. Hawkins, P. Jacobs, M. E. Mann, S. K. Miller, et al. (2015),  
192 Robust comparison of climate models with observations using blended land air and  
193 ocean sea surface temperatures, *Geophys. Res. Lett.*, 42, 6526-6534, doi:  
194 10.1002/2015GL064888.
- 195 Dessler, A. E., T. Mauritsen, & B. Stevens (2018), The influence of internal variability on  
196 Earth's energy balance framework and implications for estimating climate sensitivity,  
197 *Atmos. Chem. Phys.*, 18, 5147-5155, doi: 10.5194/acp-18-5147-2018.
- 198 Forster, P. M., T. Andrews, P. Good, J. M. Gregory, L. S. Jackson, & M. Zelinka (2013),  
199 Evaluating adjusted forcing and model spread for historical and future scenarios in the  
200 CMIP5 generation of climate models, *Journal of Geophysical Research: Atmospheres*,  
201 118, 1139-1150, doi: 10.1002/jgrd.50174.

202 Forster, P. M., T. Richardson, A. C. Maycock, C. J. Smith, B. H. Samset, G. Myhre, et al. (2016),  
 203 Recommendations for diagnosing effective radiative forcing from climate models for  
 204 CMIP6, *J. Geophys. Res.*, 121, 12460-12475, doi: 10.1002/2016jd025320.

205 Giorgetta, M. A., J. Jungclaus, C. H. Reick, S. Legutke, J. Bader, M. Böttinger, et al. (2013),  
 206 Climate and carbon cycle changes from 1850 to 2100 in MPI-ESM simulations for the  
 207 Coupled Model Intercomparison Project phase 5, *Journal of Advances in Modeling Earth*  
 208 *Systems*, 5, 572-597, doi: 10.1002/jame.20038.

209 Gregory, J. M., & P. M. Forster (2008), Transient climate response estimated from radiative  
 210 forcing and observed temperature change, *J. Geophys. Res.*, 113, doi:  
 211 10.1029/2008jd010405.

212 Hansen, J., M. Sato, R. Ruedy, L. Nazarenko, A. Lacis, G. A. Schmidt, et al. (2005), Efficacy of  
 213 climate forcings, *Journal of Geophysical Research: Atmospheres*, 110, doi:  
 214 10.1029/2005JD005776.

215 Hawkins, E., R. S. Smith, J. M. Gregory, & D. A. Stainforth (2016), Irreducible uncertainty in  
 216 near-term climate projections, *Climate Dynamics*, 46, 3807-3819, doi: 10.1007/s00382-  
 217 015-2806-8.

218 Hedemann, C., T. Mauritsen, J. Jungclaus, & J. Marotzke (2017), The subtle origins of  
 219 surface-warming hiatuses, *Nature Clim. Change*, 7, 336-339, doi:  
 220 10.1038/nclimate3274.

221 Huber, M., U. Beyerle, & R. Knutti (2014), Estimating climate sensitivity and future  
 222 temperature in the presence of natural climate variability, *Geophys. Res. Lett.*, 41, 2086-  
 223 2092, doi: 10.1002/2013GL058532.

224 Kummer, J. R., & A. E. Dessler (2014), The impact of forcing efficacy on the equilibrium  
 225 climate sensitivity, *Geophys. Res. Lett.*, 41, 3565-3568, doi: 10.1002/2014gl060046.

226 Lewis, N., & J. A. Curry (2015), The implications for climate sensitivity of AR5 forcing and  
 227 heat uptake estimates, *Climate Dynamics*, 45, 1009-1023, doi: 10.1007/s00382-014-  
 228 2342-y.

229 Lewis, N., & J. Curry (2018), The impact of recent forcing and ocean heat uptake data on  
 230 estimates of climate sensitivity, *J. Climate*, doi: 10.1175/jcli-d-17-0667.1.

231 Marvel, K., G. A. Schmidt, R. L. Miller, & L. S. Nazarenko (2015), Implications for climate  
 232 sensitivity from the response to individual forcings, *Nature Climate Change*, 6, 386, doi:  
 233 10.1038/nclimate2888.

234 Mauritsen, T., & R. Pincus (2017), Committed warming inferred from observations, *Nature*  
 235 *Climate Change*, 7, 652-655, doi: 10.1038/nclimate3357.

236 Morice, C. P., J. J. Kennedy, N. A. Rayner, & P. D. Jones (2012), Quantifying uncertainties in  
 237 global and regional temperature change using an ensemble of observational estimates:  
 238 The HadCRUT4 data set, *J. Geophys. Res.*, 117, doi: 10.1029/2011jd017187.

239 Otto, A., F. E. L. Otto, O. Boucher, J. Church, G. Hegerl, P. M. Forster, et al. (2013), Energy  
 240 budget constraints on climate response, *Nature Geoscience*, 6, 415-416, doi:  
 241 10.1038/ngeo1836.

242 Richardson, M., K. Cowtan, E. Hawkins, & M. B. Stolpe (2016), Reconciled climate response  
 243 estimates from climate models and the energy budget of Earth, *Nature Clim. Change*, 6,  
 244 931-935, doi: 10.1038/nclimate3066.

245 Santer, B. D., T. M. L. Wigley, D. J. Gaffen, L. Bengtsson, C. Doutriaux, J. S. Boyle, et al. (2000),  
 246 Interpreting differential temperature trends at the surface and in the lower  
 247 troposphere, *Science*, 287, 1227.



248 Shindell, D. T. (2014), Inhomogeneous forcing and transient climate sensitivity, Nature  
249 Climate Change, 4, 274, doi: 10.1038/nclimate2136.  
250

251  
252

**Table 1. TCR<sub>hist</sub> calculated with different base and end periods**

base period	end period	average (K)	Full TCR range (K)	5-95% TCR range (K)	width (K)	% diff from true TCR	ΔF (W/m <sup>2</sup> )
1859-1882	1940-1949	1.82	0.63-2.88	1.15-2.50	1.35	0.4	0.54
1859-1882	1951-1960	1.96	1.10-3.13	1.32-2.67	1.34	7.6	0.59
1859-1882	1969-1978	1.71	1.01-2.91	1.24-2.24	0.99	-5.8	0.81
<b>1859-1882</b>	<b>1996-2005</b>	<b>1.68</b>	<b>1.32-1.94</b>	<b>1.48-1.90</b>	<b>0.42</b>	<b>-7.7</b>	<b>1.85</b>
1930-1939	1996-2005	1.65	0.97-2.07	1.35-1.99	0.64	-9.7	1.41
1940-1949	1996-2005	1.62	1.02-2.16	1.28-2.04	0.76	-11.5	1.31
1951-1960	1996-2005	1.55	0.91-2.04	1.20-1.90	0.70	-16.8	1.26
1970-1979	1996-2005	1.67	0.99-2.42	1.20-2.09	0.90	-8.5	0.99

253 The bold line is the case primarily discussed in the text. Width is the difference between the 5<sup>th</sup> and 95<sup>th</sup>  
254 percentile values; % difference is average TCR<sub>hist</sub> minus TCR<sub>true</sub>, 1.81 K, divided by average TCR<sub>hist</sub>, in  
255 percent; ΔF is the change in forcing between the base and end periods.

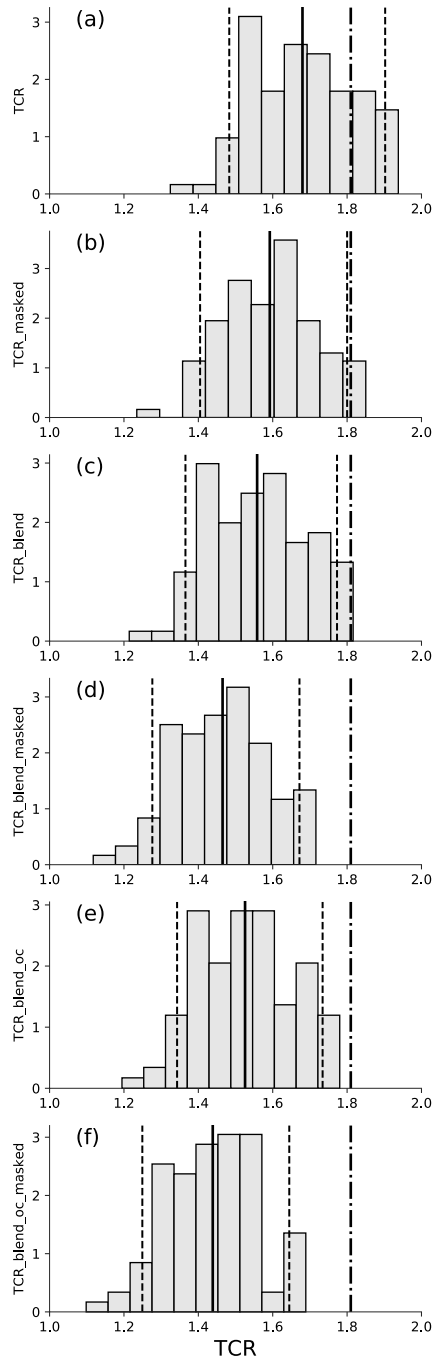
256  
257

**Table 2. TCR<sub>hist</sub> calculated with different versions of ΔT**

ΔT <sub>s</sub>		average (K)	5-95% TCR range (K)	% diff from True TCR
TCR	<b>ΔT is global-average near-surface air temperature</b>	<b>1.68</b>	<b>1.48-1.90</b>	<b>-7.7</b>
TCR_masked	Same as TCR, but geographic coverage follows HadCRUT4	1.59	1.40-1.80	-13.7
TCR_blend	ΔT is a blend of near-surface air temperature over land and sea ice and SSTs over open ocean	1.56	1.37-1.77	-16.2
TCR_blend_masked	Same as TCR_blend, but geographic coverage follows HadCRUT4	1.47	1.28-1.67	-23.5
TCR_blend_oc	ΔT is a blend of near-surface air temperature over land and sea ice; elsewhere, use temperature of the top 12 m of the ocean	1.53	1.34-1.73	-18.6
TCR_blend_oc_masked	Same as TCR_blend_oc, but geographic coverage follows HadCRUT4	1.44	1.25-1.64	-25.8

258 The bold line is the base case primarily discussed in the text; % difference is average TCR<sub>hist</sub> minus  
259 TCR<sub>true</sub>, 1.81 K, divided by average TCR<sub>hist</sub>, in percent.

260  
261



262

263 Figure 1. Histograms of  $TCR_{hist}$  (K) from the ensemble. Each panel shows the calculation with a  
264 different version of  $\Delta T$ ; see Table 2 for definitions. The solid black line represents the average,  
265 the dashed lines are the 5<sup>th</sup> and 95<sup>th</sup> percentiles. The dot-dashed line is  $TCR_{true}$  of the model,  
266 1.81 K.